The 10th International Symposium on Flow Visualization
August 26-29, 2002, Kyoto, Japan
F0095

Visualized Numerical Three-Dimensional Flow Development between Very Short Rotating Cylinders

Umemura, N. *[1], Watanabe, T. *[2], Furukawa, H. *[3] and Nakamura, I. *[4]

*1 Graduate School of Human Informatics, Nagoya University,
Nagoya 464-8601 Japan
Tel: +81-52-789-4862 / Fax: +81-52-789-4802
E-mail: umemura@view.human.nagoya-u.ac.jp
*2 Center for Information Media Studies, Nagoya University
*3 Fuji Research Institute Corporation
*4 Department of Mechanical Engineering, Meijo University

Abstract: The investigation of Taylor-Couette flow developing between two rotating concentric cylinders gives an interesting point in the nonlinear dynamics and transient dynamics. When the aspect is around 0.1 to 1.5, and the outer cylinder is at rest and the inner cylinder is suddenly accelerated from rest to a constant angular velocity, the four modes of final flows appear: the normal 2-cell mode, anomalous 1-cell mode, twin-cell mode and alternate mode. The alternate mode appears at the aspect ratio about unity. The alternate mode has four types that are specified by the volume-averaged enstrophy, and each type shows its own time-dependent developing processes.

Keywords: Taylor-Couette Flow, Short Annulus, Nonlinear Phenomenon, Mode Transition, Three Dimensional Calculation

1. Introduction

Taylor-Vortex flow developing between two-concentric cylinders has a variety of flow patterns, and the flow modes and mode bifurcations have been investigated from the experimental and numerical point of views.

When the length of cylinders is finite, the end walls of cylinders have a great effect on the formation processes of final flow patterns (Benjamin and Mullin, 1981). Even when the length of cylinders is the same order of magnitude of the gap width between cylinders, various flow modes have been found experimentally (Benjamin, 1981, Buzug, 1992) and numerically (Pfister, 1988, Magère 2000). The detail experiment (Nakamura and Toya, 1996) showed that more flow modes appeared. In these studies, the main purpose is the investigation of the fully developed flows, and the unsteady processes of the flow pattern formations are not well covered. Furukawa et al. (Furukawa 2002) numerically investigated the mode formation processes of the axisymmetric flows. They predicted the flow patterns found by Nakamura and Toya, and they also showed a new mode that was not steady. However, for the flow with the aspect ratio about unity, the formation process or the three-dimensional flow is not investigated.

In this paper, we use the three-dimensional numerical scheme in order to study Taylor-Vortex flow between rotating inner and stationary outer cylinders with very short annulus. Initially, the fluid is at rest and the inner cylinder suddenly starts to rotate at a constant angular velocity. The time-dependent process of the mode formation and final flow modes at various Reynolds numbers are predicted.

Copyright © 2002 by VSJ

2. Governing Equations and Numerical Method

The radii of inner and outer cylinders are R_i and R_o, respectively, and the gap width of the cylinder D is $R_o - R_i$. The length of cylinders is L and the aspect ratio Γ is defined by L/D. The reference length is D and the reference velocity is the circumferential velocity of the inner cylinder, and the Reynolds number Re is based on these reference values, that is $Re = \omega R_i D/\nu$. In this study, the radius ratio η (= R_i / R_o) is set to be 0.667. The governing equations are the Navier-Stokes equations and the equation of continuity in the cylindrical coordinate system (r, θ, z),

$$\frac{\partial \boldsymbol{u}}{\partial t} + (\boldsymbol{u}\cdot\nabla)\boldsymbol{u} = -\nabla p + \frac{1}{Re}\nabla^2 \boldsymbol{u}, \tag{1}$$

$$\nabla\cdot\boldsymbol{u} = 0, \tag{2}$$

where t is the time, $\boldsymbol{u}$ is the velocity vector with components (u, v, w), p is the pressure. We introduce a function ψ and integrate ψ to visualize flow in the meridional section,

$$u = -\frac{1}{r}\frac{\partial \psi}{\partial z}. \tag{3}$$

If the flow is axisymmeric, ψ is Stokes' stream function. But in general ψ is a tool for flow visualization.

The basic solution method is the marker and cell method. The convection terms are discretized by the QUICK method, and other terms are formulated by the second-order central difference method. The time integration is the Euler explicit method. The spatial grid is the staggered grid, and the numbers of grid points in the radial direction and the circumferential direction are 40 and 36, respectively. The grid point in the axial direction is determined by the proportionality to the cylinder length with 40 points for the aspect ratio of unity. The initial velocity is zero in the entire region and the boundary condition of velocity components is the non-slip condition.

The axisymmery of the flow is estimated by the spatial variance of the circumferential velocity,

$$V(r,t) = \frac{1}{L}\int_0^L \frac{1}{2\pi r}\int_0^{2\pi}\left\{v - \frac{1}{2\pi r}\int_0^{2\pi} v\, r d\theta\right\}^2 r\, d\theta dz. \tag{4}$$

When the value of $V(r, t)$ at r = 2.1125 is less than $5.0\text{x}10^{-5}$, we determine that the flow is axisymmetic, and the flow is wavy otherwise.

The total torque on the outer cylinder is given by

$$N(t) = \int_0^{2\pi}\int_0^L R_o^2 \mu\left(r\frac{\partial}{\partial r}\left(\frac{v}{r}\right) + \frac{1}{r}\frac{\partial u}{\partial \theta}\right) dz d\theta, \tag{5}$$

and the flow is steady when the relative time variation of N is less than 10^{-4}, and it is unsteady otherwise.

In order to investigate the global development of the flow, we use the volume-averaged enstrophy Ω and the kinetic energy E,

$$\Omega = \frac{1}{A}\int_{R_i}^{R_0}\int_0^{2\pi}\int_0^L \frac{1}{2}\left(\frac{\partial u}{\partial z} - \frac{\partial w}{\partial r}\right)^2 r\, dz d\theta dr, \tag{6}$$

$$E = \frac{1}{A}\int_{R_i}^{R_0}\int_0^{2\pi}\int_0^L \frac{1}{2}\boldsymbol{u}^2\, r\, dz d\theta dr, \tag{7}$$

where A is the total volume of the annulus.

Copyright © 2002 by VSJ

3. Results

3.1 Mode of Fully Developed Flows

Figure 1 shows the final modes of the fully developed flows. The modes appeared are the normal 2-cell mode (N2), anomalous 1-cell mode (A1), twin-cell mode (Twin) and alternate mode (Alternate). The flows near the end walls in the normal 2-cell mode are inward and the flow directs fluid from the outer cylinder to the inner cylinder. The anomalous 1-cell mode has a large cell (vortex) and an outward flow near the upper or lower end wall. The twin-cell mode found by the experiment (Nakamura and Toya, 1996) has two large cells in the radial direction. The alternate mode is the time-dependent mode that shows a periodic growth and decay of each cell. The red thick line in Fig. 1 is the boundary that separates the axisymmetric flows and asymmetric wavy flows.

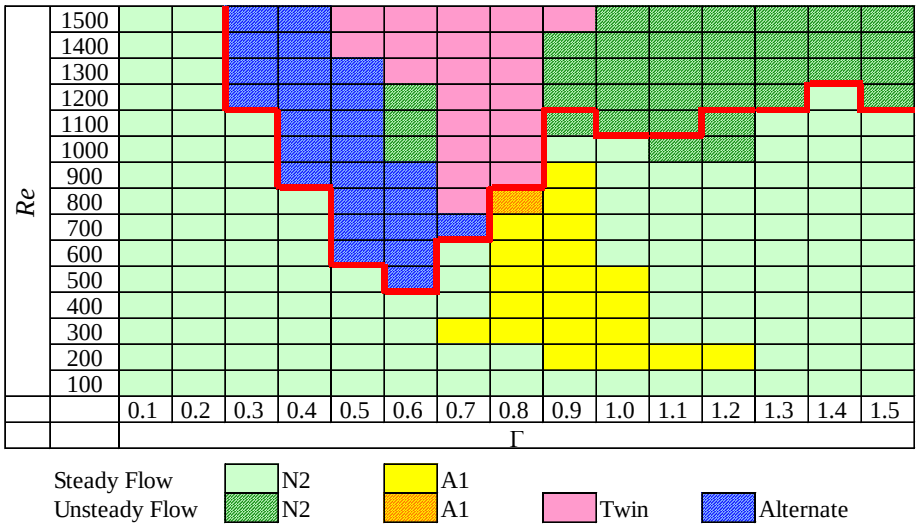

Fig. 1 Fully Developed Flow Patterns Obtained by Three-Dimensional Numerical Calculations

3.2 Mode Formation Processes

The four fully developed flow modes shown in Sec. 3.1 are formed via the normal 2-cell mode. The development of the anomalous 1-cell mode was given by Furukawa et al. (Furukawa, 2002).
The formation processes of the twin-cell mode are shown in Figs. 2, 3. Figure 2 and Fig. 3(a) are the contours of the value of the function ψ, and the inner cylinder is on the left side and the outer cylinder is on the right side. Movie 1 shows the three-dimensional contour of the function ψ at Γ = 0.7, Re = 800 and t = 0 to 562. Movie 2 shows the contour of the function ψ at Γ = 0.7, Re = 1500 and t = 0 to 562. Figure 3(b) is the contours of the circumferential velocity component in the (r, θ) plane. In these figures, the mean value is represented by green, and the larger and smaller values are shown by warmer and cooler color, respectively. One cell collapses and divides other cell, and the divided cells move to the inner and outer sides of cylinders. While the inner cell forms an extra cell, the outer cell grows again and the twin-cell mode that has two large cells in the radial direction appears (Fig. 2, t = 214. Fig. 3(a), t = 186). When the Reynolds number is higher, two cells oscillate, as shown in Fig. 3(a), t = 90 to 129. This oscillation is asymmetric, as we will see later.

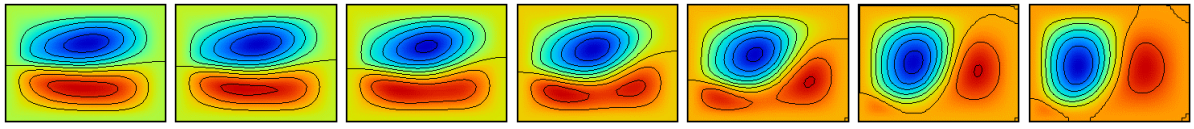

Fig. 2 Flow Development from Normal 2-cell Mode to Twin-cell Mode (Γ = 0.7, Re = 800, $\theta = \pi / 3$)

Copyright © 2002 by VSJ

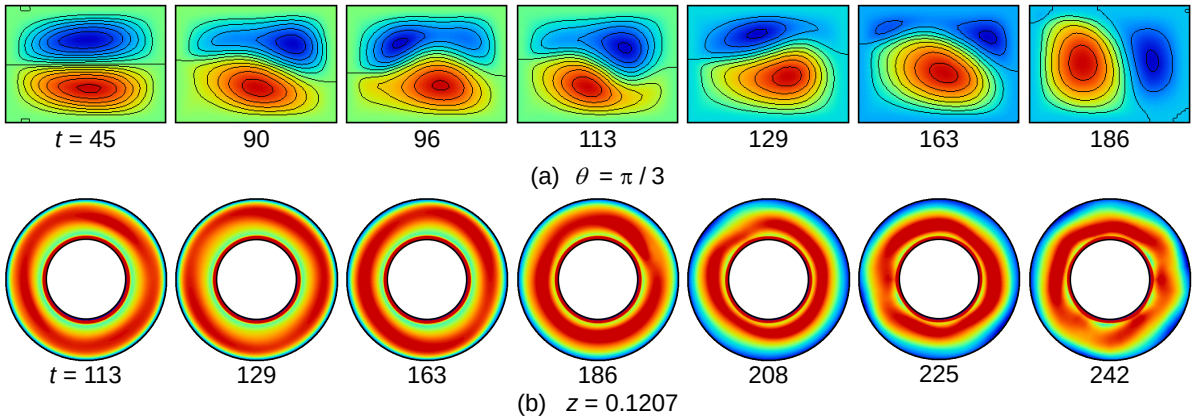

Fig. 3 Flow Development from Normal 2-cell Mode to Twin-cell Mode (Γ = 0.7, Re = 1500)

The development to the alternate mode flow is shown in Fig. 4 and Movie 3. The formation of the alternate mode begins with the collapsing of the normal two cells with each other. The flow has the 2-cell mode at the earlier time (t = 191), and one cell breaks the other cell into two cells as time goes on. The broken cells are convected toward the inner and the outer cylinder sides, and three cells appear (t = 225). As the time passes further, the broken cells merge and the 2-cell mode is formed (t = 248). The exchange between the 2-cell mode and the flow with three cells continues for a while. Then, the governing cell appears and collapses the other cell, while it breaks itself and four cells appear (t = 259).

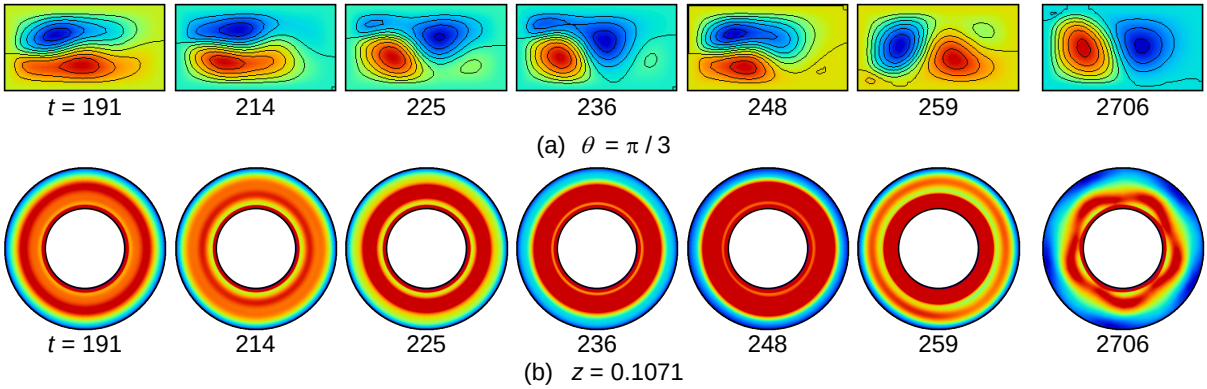

Fig. 4 Flow Development from Normal 2-cell Mode to Alternate Mode (Γ = 0.5, Re = 1200)

Figure 5 shows the time variation of the variance $V(r, t)$ at r = 2.1125. The formation process of the anomalous 1-cell mode (A1) is axisymmetric. When the flow is the twin-cell mode and the Reynolds number is low (Re = 800), the variance increases just after the twin-cell mode is formed (Fig. 2, t = 214). When the Reynolds number is higher (Re = 1500), the variance grows before the twin-cell mode appears (Fig. 3(a), t = 45). At any Reynolds number, when the flow is the alternate mode, the variance increases after the flow mode is established. When the Reynolds number is lower (Re = 500), the growth of the variance of the alternate mode is gradual and periodic, and the flow exchange between the axisymmetic flow and the asymmetric flow is found. At the higher Reynolds number (Re = 1200), the variance increases rapidly after the mode exchange.

Copyright © 2002 by VSJ

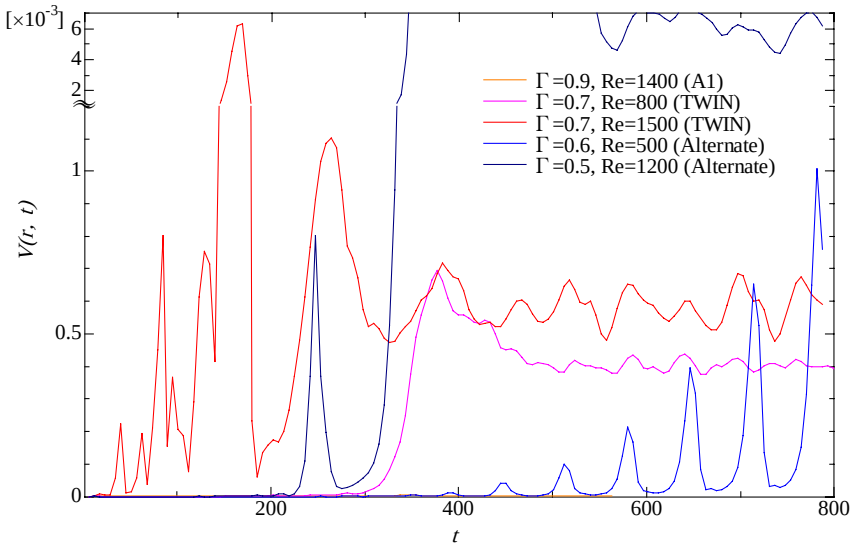

Fig. 5 Time Variation of Variance of Circumferentional Velocity (r = 2.1125)

3.3 Alternate Mode

The numerical investigation of the axisymmetric flow carried out by Furukawa et al. (Furukawa, 2002) showed the periodic time-variation of the volume-averaged enstrophy. In the present calculation, not the completely periodic variation is obtained but the quasi-periodic variation is found. Other than the quasi-periodic variation, three types are found: the type in which the value of the enstrophy suddenly decreases, the type in which the variation accompanies beats and the type in which no periodicity appears. Therefore, the alternate modes are classified into four types. These types are characterized by the time-variations of the mean enstrophy and energy.

(a) *type 1*

In the alternate mode of type 1, the amplitude and the wavelength of the time variation of the enstrophy are not completely constant, though cells collapse with each other. Figure 6 shows the variations of the enstrophy and energy at $\Gamma = 0.5$ and $Re = 600$. The oscillations of the variations appear when the symmetric normal 2-cell mode initially formed begins to deform ($t = 250$). This behavior initiates the alternate mode, and the motion with almost constant amplitude continues. At $t = 1200$ when the wavy flow begins to grow and the value of $V(r, t)$ increases rapidly, the amplitudes of the variations of the enstrophy and energy start to decrease, and then they remain almost constant at $t = 2000$. In these variations, cells align in the axial direction at their maxima, and cells align in the radial direction at their minima. One period of the variation of cells' formation corresponds to the two periods of the variation of the enstrophy, and it is coincident with the result obtained by Furukawa et al. (Furukawa, 2002).

Copyright © 2002 by VSJ

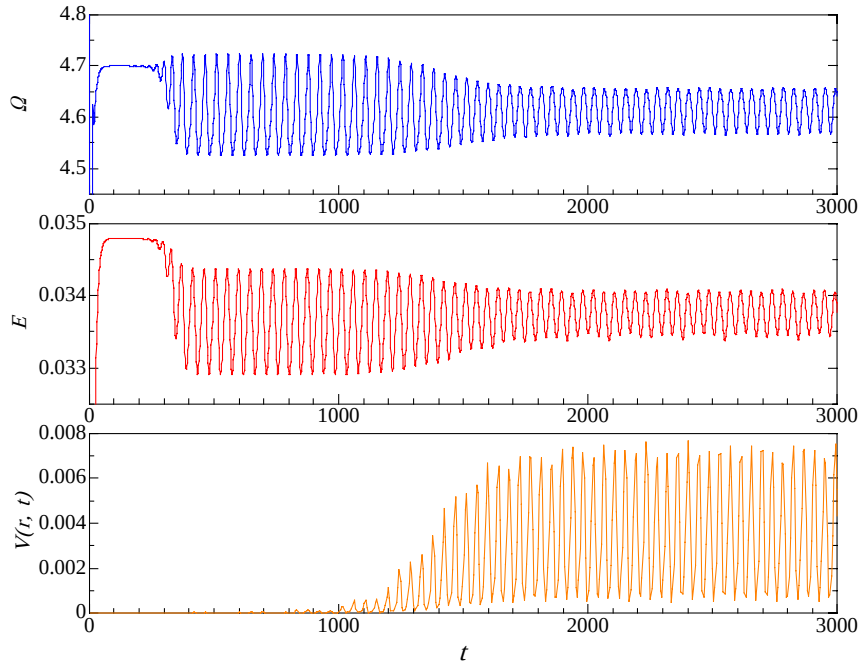

Fig. 6 Time Variations of Enstrophy, Energy and Variance (Γ = 0.5, *Re* = 600, *r* = 2.1125)

(b) *type 2*

In type 2, the enstrophy and the enrgy show small variations after their rapid decreases. The time changes at Γ = 0.6 and *Re* = 900 are shown in Fig. 7. The amplitudes of the enstrophy and the energy once grow and the wavy flow appears when the two normal cells begin to collapse each other (t = 400). After t = 700, the variance $V(r, t)$ becomes small and the magnitude of the enstrophy and energy remains small order.

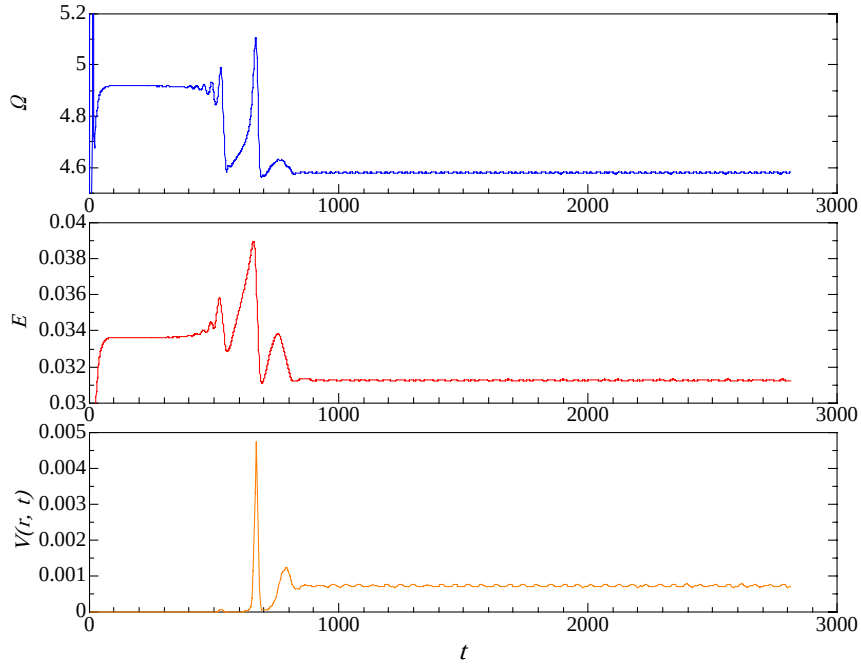

Fig .7 Time Variations of Enstrophy, Energy and Variance (Γ = 0.6, *Re* = 900, *r* = 2.1125)

Copyright © 2002 by VSJ

The detail of the transition during which the variation of enstrophy decreases is shown in Fig. 8, and the contours of ψ are shown in Fig. 9. At a minimum of the variation (t = 551), four cells align in the radial direction. As the enstrophy increases, the second and the fourth cells from the inner wall, and the first and the third cells from the inner wall merge (t = 647), the cells align in the axial direction when the variation reaches its maximum (t = 664). After t = 664 and the enstrophy decreases, the lower cell collapses the upper cell (t = 675), and the value of the enstrophy shows its minimum when the cells align in the radial direction (t = 686). As the time passes by further, the enstrophy begins to grow once again and reaches its maximum (t = 759), though the increase is not larger than that at t = 664 and no rearrangement of cells' formation occurs. That is, after t = 686, the collapses of cells are not found. Finally, a small variation continues while cells align in the radial direction.

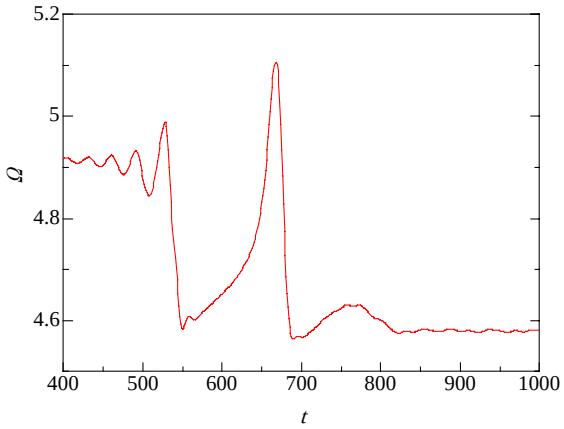

Fig. 8 Time Variation of Enstrophy (Γ = 0.6, Re = 900)

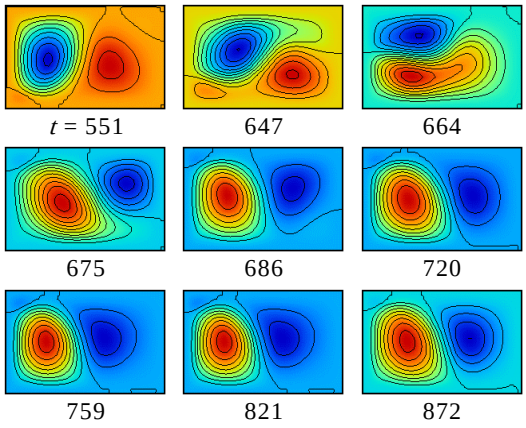

Fig. 9 Contours of ψ in r-z Plane (Γ = 0.6, Re = 900, $\theta = \pi / 3$)

(c) *type 3*

In type 3, the variations of the enstrophy and the energy have some beats before they remain in quasi-periodic states. Figure 10 shows the variations at Γ = 0.4 and Re = 1000. When the cells in the normal 2-cell mode firstly begin to collapse each other (t = 200), the variations have large amplitudes and the alternate mode appears. Cells align in the axial direction at the maxima of the variation and in the radial direction at the minima. The amplitudes repeat their increases and decreases, and the flow developes with beats of the variations. Small amplitudes of the enstrophy and the energy appear around t = 1000, t = 1900 and t = 2700. At these time points, the variation V (r, t) increases and the flow is more wavy. The beats cease as time advances. Finally, the flow becomes quasi-periodic.

Copyright © 2002 by VSJ

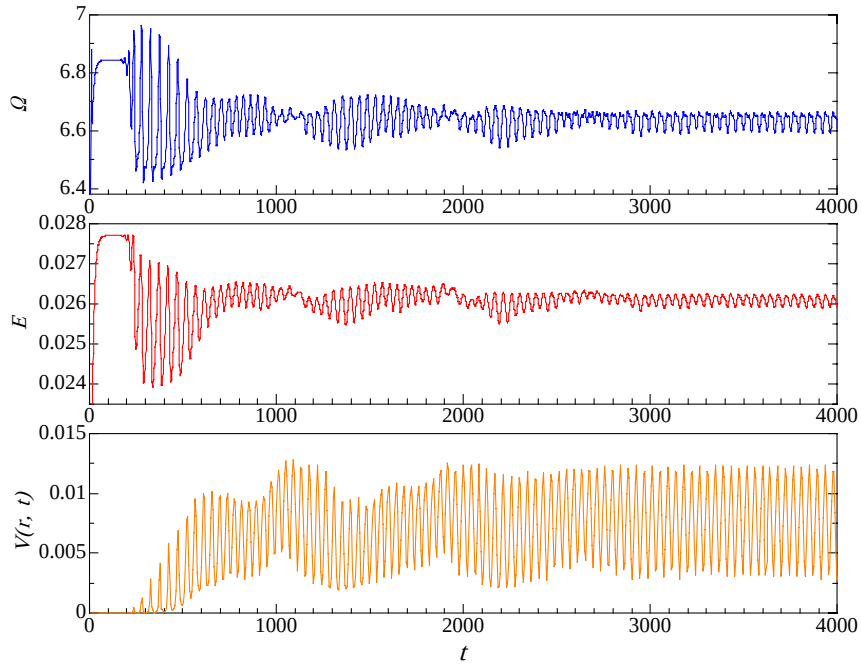

Fig. 10 Time Variations of Enstrophy, Energy and Variance (Γ = 0.4, *Re* = 1000, *r* = 2.1125)

(d) *type 4*

The variations of the enstrophy and the enrgy in type 4 have irregular changes. The variations at Γ = 0.4 and *Re* = 1300 are shown in Fig. 11. At *t* = 200, the initially formed 2-cell mode flow begins to deform, and the amplitudes of variations increase. After $V(r, t)$ grows beyond the criterion of the wavy flow, the variations of the enstrophy, energy and variance are not periodic. When the amplitude of the variation is large, cells align in the axial direction at maxima of the variation and in the radial direction at minima. Some correspondences between the variations of the enstrophy and the energy are found, though it is not complete.

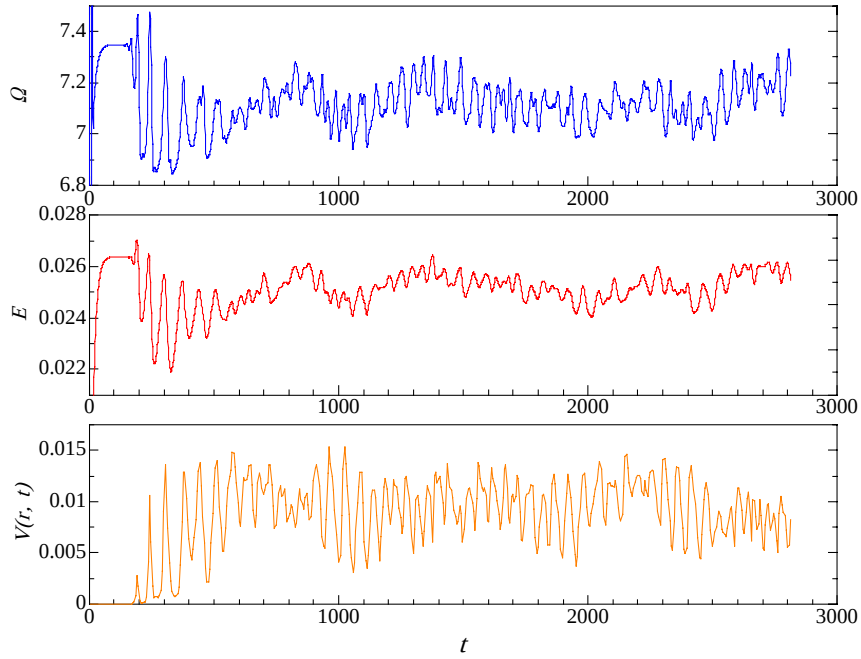

Fig. 11 Time Variations of Enstrophy, Energy and Variance (Γ = 0.4, *Re* = 1300, *r* = 2.1125)

Copyright © 2002 by VSJ

Figure 12 represents the region in the (Γ, *Re*) plane, where each type of the alternate mode appears. Flows with quasi-periodic variations of the enstrophy (type 1) appear at smaller Reynolds numbers, while the region where flows with rapid decreases in the variations (type 2) emerges at higher Reynolds numbers and it is neighboring to the regions of the normal two-cell mode and the twin-cell mode. The flows with irregular variations (type 4) are formed smaller aspect ratios.

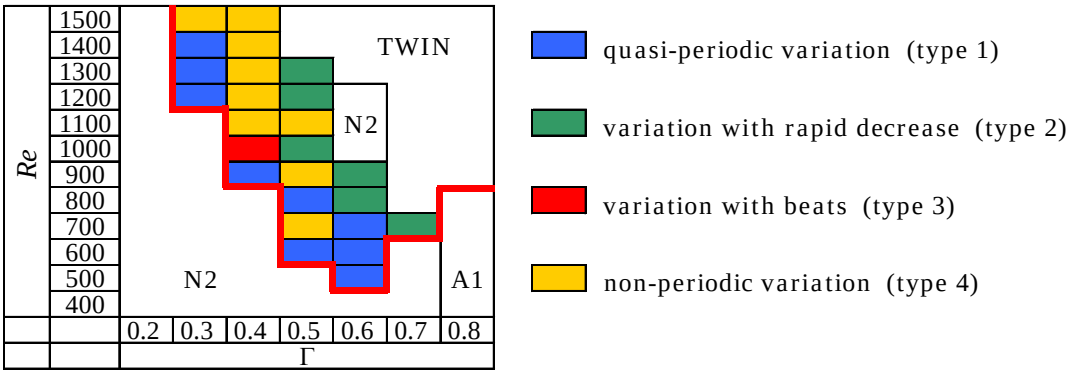

Fig. 12 Diagram of Four Types of Alternate Mode

4. Summary

The three-dimensional numerical investigation is carried out on the flow between rotating inner and stationary outer cylinders with finite length. The flow starts suddenly from rest, and the fully developed flow and the process of the mode formation are analyzed by newly introducing the variance of the circumferentional velocity.

Four modes appear at the fully developed flows: the normal 2-cell mode, anomalous 1-cell mode, twin-cell mode and alternate mode.

The formation process of the anomalous 1-cell mode is axisymmetric.

When the flow at smaller Reynolds number has the twin-cell mode, the flow develops from the symmetric normal 2-cell mode and it becomes wavy after the twin-cell mode is established. At higher Reynolds number, the asymmetric normal two cells collapse each other and the flow becomes wavy before the twin-cell mode appears.

In the alternate mode, two asymmetric cells break each other at the first process. The final flow of the alternate mode is wavy at any Reynolds number. The alternate mode has four types of its developments. The type 1 shows the quasi-periodic variations of the volume-averaged enstrophy and energy, and the type 2 has rapid decreases in the variations. The variations accompany beats in the type 3, and no regularity of variations is found in the type 4. Cells in flows tend to align in the axial direction at the maxima of the variation of the enstrophy and align in the radial direction at the minima.

List of Movies

Movie 1: Three-Dimensional contour of the function ψ at $\Gamma = 0.7$, $Re = 800$ and $t = 0$ to 562 (1117kB)

Movie 2: Three-Dimensional contour of the function ψ at $\Gamma = 0.7$, $Re = 1500$ and $t = 0$ to 562 (1160kB)

Movie 3: Three-Dimensional contour of the function ψ at $\Gamma = 0.5$, $Re = 1200$ and $t = 0$ to 562 (1079kB)

Copyright © 2002 by VSJ

References

Benjamin, T.B., Mullin, T., 1981, “Anomalous mode in the Taylor experiment,” Proc. Royal Soc. Lnd., A, Vol. 377, 221.

Buzug, Th., von Stamm, J., Pfister, G., 1992, “Fractal dimensions of strange attractors obtained from the Taylor-Couette experiment,” Physica A, Vol. 191, 559.

Pfister, G., Schmidt, H., Cliffe, K.A., Mullin, T., 1988, “Bifurication phenomena in Taylor-Couette flow in a very short annulus,” J. Fluid Mech., Vol. 191, 1.

Magère, E., Deville, M.O., 2000, “Simulation of the Taylor-Couette flow in a finite geometry by spectral element method,” Appl. Numer. Math., Vol. 33, 241.

Nakamura, I., Toya, Y., 1996, “Existance of extra vortex and twin vortex of anomalous mode in Taylor vortex flow with a small aspect ratio,” Acta Mechanica, Vol. 117, 33.

Furukawa, H., Watanabe, T., Toya, Y., Nakamura, I., 2002, “Flow pattern exchange in the Taylor-Couette system with a very small aspect ratio,” Phys. Rev. E, Vol. 65, 036306.

Copyright © 2002 by VSJ